*materials*

MDPI

*Article*

# Investigation of the Itinerant Electron Ferromagnetism of $Ni_{2+x}MnGa_{1-x}$ and $Co_2VGa$ Heusler Alloys

**Takuo Sakon [1,*], Yuhi Hayashi [1], Akihito Fukuya [1], Dexin Li [2], Fuminori Honda [2], Rie Y. Umetsu [3], Xiao Xu [4], Gendo Oomi [5], Takeshi Kanomata [6] and Tetsujiro Eto [5]**

1 Department of Mechanical and Systems Engineering, Faculty of Science and Technology, Ryukoku University, Otsu, Shiga 520–2194, Japan; t150289@mail.ryukoku.ac.jp (Y.H.); t150299@mail.ryukoku.ac.jp (A.F.)
2 Institute for Materials Research, Tohoku University, Oarai, Ibaraki 311–1313, Japan; dxli@imr.tohoku.ac.jp (D.L.); honda@imr.tohoku.ac.jp (F.H.)
3 Institute for Materials Research, Tohoku University, Sendai, Miyagi 980–8577, Japan; rieume@imr.tohoku.ac.jp
4 Department of Materials Science, Graduate School of Engineering, Tohoku University, Sendai, Miyagi 980–8579, Japan; xu@material.tohoku.ac.jp
5 Kurume Institute of Technology, Kurume, Fukuoka 830–0052, Japan; geomi@kurume-it.ac.jp (G.O.); teto@kurume-it.ac.jp (T.E.)
6 Research Institute for Engineering and Technology, Tohoku Gakuin University, Tagajo, Miyagi 985–8537, Japan; kanomata@mail.tohoku-gakuin.ac.jp
* Correspondence: sakon@rins.ryukoku.ac.jp; Tel.: +81-77-543-7443

Received: 20 January 2019; Accepted: 12 February 2019; Published: 14 February 2019


**Abstract:** Experimental investigations into the field dependence of magnetization and temperature dependences of magnetic susceptibility in $Ni_{2+x}MnGa_{1-x}$ ($x$ = 0.00, 0.02, 0.04) and $Co_2VGa$ Heusler alloy ferromagnets were performed following the spin fluctuation theory of itinerant ferromagnetism, called as "Takahashi theory". We investigated the magnetic field dependence of magnetization at the Curie temperature $T_C$, which is the critical temperature of the ferromagnetic–paramagnetic transition, and also at $T$ = 5 K, which concerns the ground state of the ferromagnetic state. The field dependence of the magnetization was analyzed by means of the $H$ vs. $M^5$ dependence, and the field dependence of the ground state at 5 K was investigated by means of an Arrott plot ($H/M$ vs. $M^2$) according to the Takahashi theory. As for $Ni_{2+x}MnGa_{1-x}$, the spin fluctuation parameter in $k$-space (momentum space, $T_A$) and that in energy space ($T_0$) obtained at $T_C$ and 5 K were almost the same. On the contrary, as for $Co_2VGa$, the $H$ vs. $M^5$ dependence was not shown at $T_C$. We obtained $T_A$ and $T_0$ by means of an Arrott plot at 5 K. We created a generalized Rhodes–Wohlfarth plot of $p_{eff}/p_S$ versus $T_C/T_0$ for the other ferromagnets. The plot indicated that the relationship between $p_{eff}/p_S$ and $T_0/T_C$ followed Takahashi's theory. We also discussed the spontaneous magnetic moment at the ground state, $p_S$, which was obtained by an Arrott plot at 5 K and the high temperature magnetic moment, $p_C$, at the paramagnetic phase. As for the localized ferromagnet, the $p_C/p_S$ was 1. As for weak ferromagnets, the $p_C/p_S$ was larger than 1. In contrast, the $p_C/p_S$ was smaller than 1 by many Heusler alloys. This is a unique property of Heusler ferromagnets. Half-metallic ferromagnets of $Co_2VGa$ and $Co_2MnGa$ were in accordance with the generalized Rhodes–Wohlfarth plot with a $k_m$ around 1.4. The magnetic properties of the itinerant electron of these two alloys appeared in the majority bands and was confirmed by Takahashi's theory.

**Keywords:** ferromagnetic Heusler alloy; magnetization; itinerant electron ferromagnetism; half-metal

## 1. Introduction

Spin fluctuation theories have been proposed to explain the physical principles of the itinerant electron system [1–7]. Takahashi proposed the self-consistent renormalization (SCR) theory according to zero-point spin fluctuations, which assimilated both the transverse and longitudinal components of the fluctuations [4–7]. An outstanding characteristic of this theory is the magnetization at $T_C$. The theory proposed by Takahashi indicates that the magnetic field dependence, $H$, is proportional to the magnetization, $M^5$, at the Curie temperature, $T_C$. This property was obtained by the differential calculus of the magnetization of the spin fluctuation free energy [7–9].

In this theory, the relation between the magnetic fields $H$ and magnetization $M$ is obtained theoretically by the equation of,

$$H = c(T_C)M^5 \tag{1}$$

where $c$ ($T_C$) is the constant value at $T_C$ (refer to the references for the derivation process of Equation (1) [7,9]). MnSi [10], $Fe_xCo_{1-x}Si$ [11], $CoS_2$ [12], and Ni [13] followed the relationship provided in Equation (1). The Heusler isotropic ferromagnetic alloy $Ni_{2+x}MnGa_{1-x}$ ($x$ = 0.00, 0.02, 0.04) also followed the relationship mentioned in Equation (1) [8,9,13]. From the spontaneous magnetic moment and magnetization at $T_C$, we obtained the spin fluctuation parameter in $k$-space (momentum space, $T_A$) and in energy space ($T_0$).

The other approach to obtain $T_A$ and $T_0$ is the analysis of the field dependence of the magnetization by means of an Arrott plot ($H/M$ vs. $M^2$) at the ground magnetic state, $T$ = 5 K [7,14]. Tateiwa et al. mentioned the derivation method of this approach in detail [14]. The magnetization in the ground state is expressed by the following equation

$$H = \frac{F_1}{N_0^3(g\mu_B)^4} \times \left(-M_0^2 + M^2\right)M \tag{2}$$

where $g$ is Lande's g-factor; $N_0$ is Avogadro's number; and $F_1$ is the mode–mode coupling term defined as

$$F_1 = \frac{2T_A^2}{15cT_0} \tag{3}$$

where $c$ is equal to 1/2 and $M_0$ is the spontaneous magnetization. $F_1$ is derived from the slope of the Arrott plot ($H/M$ vs. $M^2$ plot) at low temperatures by Equation (4)

$$F_1 = \frac{N_0^3(2\mu_B)^4}{k_B\zeta} \tag{4}$$

where $k_B$ is the Boltzmann constant, and $\zeta$ is the slope of the Arrott plot. $T_A$ and $T_0$ are obtained by the following relations of

$$\left(\frac{T_C}{T_0}\right)^{5/6} = \frac{p_S^2}{5g^2C_{4/3}} \times \left(\frac{15cF_1}{2T_C}\right)^{1/2} \tag{5}$$

$$\left(\frac{T_C}{T_A}\right)^{5/6} = \frac{p_S^2}{5g^2C_{4/3}} \times \left(\frac{2T_C}{15cF_1}\right)^{1/2} \tag{6}$$

where $C_{4/3}$ = 1.00608, and $p_S$ is the spontaneous magnetic moment at the ground state ($T$ = 0 K). In the Takahashi theory, it is mentioned that the experimental results of the magnetization measurement can be applied to these equations in units of kOe and emu/g for the magnetic fields $H$ and magnetization $M$, respectively (p. 66 in Reference [7]). Therefore, we used these units to calculate the $T_A$ and $T_0$ parameters clearly. Incidentally, the value of the magnetic field $H$ in 10 kOe is equal to the value in T (Tesla), and the value of magnetization $M$ in emu/g is equal to the value in $Am^2/kg$.

Tateiwa et al. evaluated the parameters, $T_A$ and $T_0$, of actinide 5f electron systems which were analyzed by means of Equations (4)–(6) [14]. Tateiwa et al. also used the units of kOe and emu/g.

The relation between $p_S$, $T_C$, $T_0$, and the effective magnetic moment $p_{eff}$ in the paramagnetic phase was derived from a formula shown in Equation (3.47) in [7], as follows:

$$\frac{p_{eff}}{p_S} \approx 1.4 \times \left(\frac{T_0}{T_C}\right)^{\frac{2}{3}} \quad (7)$$

Equation (7) can be rewritten as:

$$k_m = \left(\frac{p_{eff}}{p_S}\right) \times \left(\frac{T_C}{T_0}\right)^{\frac{2}{3}} \quad (8)$$

When $k_m$ is 1.4, Equation (8) is equal to Equation (7).

In this study, experimental investigations into the field dependence of magnetization and temperature dependences of magnetic susceptibility in $Ni_{2+x}MnGa_{1-x}$ ($x$ = 0.00, 0.02, 0.04) and half-metallic ferromagnets (HMFs) of $Co_2VGa$ and $Co_2MnGa$ Heusler alloys were performed following the self-consistent renormalization (SCR) spin fluctuation theory of itinerant electron ferromagnetism by Y. Takahashi [7]. We investigated the magnetic field dependence of magnetization at the Curie temperature $T_C$, which is the critical temperature of the ferromagnetic–paramagnetic transition, and also at $T$ = 5 K, which concerns the ground state of the ferromagnetic phase. We created a generalized Rhodes–Wohlfarth plot of $p_{eff}/p_S$ versus $T_C/T_0$ for the other ferromagnets. The plot indicated that the relationship between $p_{eff}/p_S$ and $T_C/T_0$ followed Takahashi's theory. We also discussed the magnetism of Heusler alloys by comparing the spontaneous magnetic moment $p_S$ at the ground state ($T$ = 0 K) and paramagnetic magnetic moment $p_C$.

## 2. Materials and Methods

The polycrystalline samples of $Ni_{2+x}MnGa_{1-x}$ ($x$ = 0.00, 0.02, 0.04) were prepared by arc melting the constituent elements, nominally, 4N Ni, 3N Mn, and 6N Ga, several times in an Ar atmosphere. Each ingot was melted several times to ensure good homogeneity. The products from the arc melting process were sealed in an evacuated silica tube and solution heat-treatment was applied at 1123 K for 3 days. After these treatments, the sample was quenched in water. The polycrystalline sample of $Co_2VGa$ was fabricated by levitation melting after making a 66.6Co–33.4Ga (at.%) binary alloy by induction furnace melting in order to avoid the reaction of the crucible by the V element. The purity of the starting elements were 99.7% V, 3N Co, and 4N Ga. The obtained ingot was annealed at 1373 K for 3 days and quenched in water.

The magnetization measurements were performed up to 5 T by means of a SQUID magnetometer (Quantum Design Inc., San Diego, USA) at the Institute for Materials Research, Tohoku University. The permeability measurement was performed in AC magnetic fields with a frequency of 73 Hz and maximum field of ± 10 Oe. The AC magnetic fields were measured by a gaussmeter 410 (Lakeshore Cryotronix Inc., Westerville, Ohio, USA). The magnetic susceptibility measurements were performed by means of a vibrating sample magnetometer (VSM, PASCO Co. Ltd, Roseville, CA, USA), which was installed in a water-cooled electromagnet (Tamagawa Seisakusho Co. Ltd., Sendai, Japan) at Ryukoku University. The magnetic susceptibility $\chi$ in the paramagnetic phase was obtained from the temperature dependences of magnetization $M$, measured at the magnetic fields of $H$ = 0.10 T and the relation of $\chi = M/H$.

## 3. Results and Discussion

### *3.1. Results of the Magnetic Measurements of $Ni_{2+x}MnGa_{1-x}$*

Figure 1 shows the Arrott plot ($M^2$ vs. $H/M$) of: (a) $Ni_2MnGa$, and (b) $Ni_{2.04}MnGa_{0.96}$ at $T$ = 5 K. By using the slope value $\zeta$ of the Arrott plot, the parameter $F_1$ was derived by Equation (4). The spontaneous magnetic moment, $p_S$; effective moment, $p_{eff}$; Curie temperature, $T_C$; and spin

fluctuation parameters $T_A$ and $T_0$ are listed in Table 1. The obtained $T_A$ and $T_0$ by the relations of Equations (5) and (6) are also listed in Table 1. Errors of $T_A$ and $T_0$ were estimated as ±10%, which arose from the error of fitting of the Arrott plot. Within these errors, the $T_A$ and $T_0$ obtained from a low temperature and the values from $T_C$ were the same as each other.

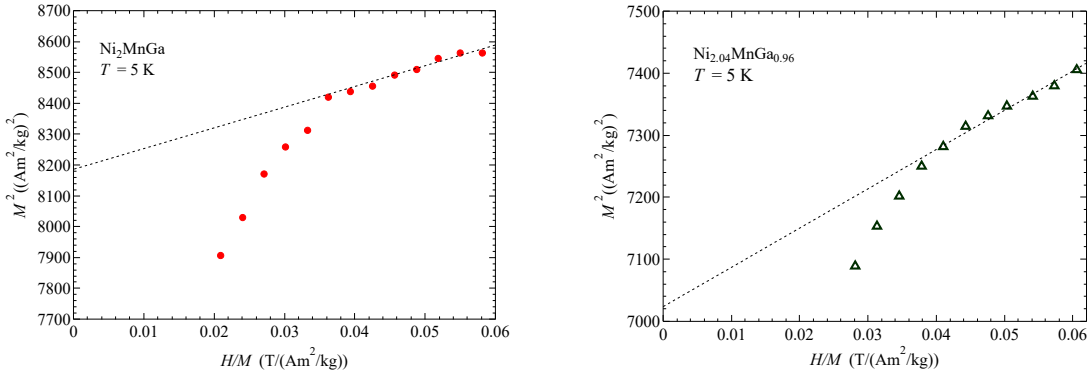


**Figure 1.** Arrott plot ($M^2$ vs. $H/M$) of: (**a**) $Ni_2MnGa$ and (**b**) $Ni_{2.04}MnGa_{0.96}$ at $T$ = 5 K.

**Table 1.** The magnetic parameters of $Ni_{2+x}MnGa_{1-x}$ ($x$ = 0.00, 0.02, 0.04). The spontaneous magnetic moment, $p_S$; effective moment, $p_{eff}$; Curie temperature, $T_C$; spin fluctuation parameter in $k$-space (momentum space) $T_A$, and that in energy space, $T_0$. The parameters $T_A$ ($T_C$) and $T_0$ ($T_C$) were obtained from the $M^4$ vs. $H/M$ plot at $T_C$ [9]. The $p_{eff}$, $T_A$ (5 K) and $T_0$ (5 K) were the obtained values in this work.

| Sample | $p_S$ ($\mu_B$/f. u.) | $p_{eff}$ ($\mu_B$/f. u.) | $T_C$ (K) | $T_A$ (K) (5 K) | $T_A$ (K) ($T_C$) [9] | $T_0$ (K) (5 K) | $T_0$ (K) ($T_C$) [9] |
|---|---|---|---|---|---|---|---|
| $Ni_2MnGa$ | 3.93 | 4.75 | 375 | 556 | 563 | 254 | 245 |
| $Ni_{2.02}MnGa_{0.98}$ | 3.79 | 4.72 | 372 | 580 | 566 | 269 | 288 |
| $Ni_{2.04}MnGa_{0.96}$ | 3.64 | 4.68 | 366 | 583 | 567 | 316 | 345 |

In a previous study, we analyzed the results of $Ni_2MnGa$ by means of the generalized Rhodes–Wohlfarth plot (double logarithmic plot of $p_{eff}/p_S$ and $T_C/T_0$) [9], which was derived to formulate the magnetic moments ratio, $p_{eff}/p_S$, and the critical temperature ratio, $T_C/T_0$. Takahashi derived an equation for the relationship between $p_S$, $T_C$, $T_0$ and the effective magnetic moment $p_{eff}$ as Equation (7). As for $Ni_2MnGa$, the measured effective moment $p_{eff}$, which was measured in this work, was 4.75, which was the same value as the result by Webster et al. [15]. For $Ni_2MnGa$, a value of 1.61 for $k_m$ was obtained by substituting a $p_{eff}$ of 4.75, and $p_S$, $T_C$, and $T_0$ from Table 1 into Equation (8).

In order to investigate the $k_m$ values of $Ni_{2+x}MnGa_{1-x}$ ($x$ = 0.02, 0.04) and compare them with other ferromagnetic alloy and compounds, we further needed $p_{eff}$ values of these alloys. We measured the magnetic susceptibility of these alloys, and $p_{eff}$ values were obtained from the Curie constant of the Curie law.

Figure 2 shows the inverse magnetic susceptibilities, $1/\chi = H/M$. The gradient of $1/\chi$ vs. $T$, which is indicated by the dotted lines, is equal to $1/C$, where $C$ is a Curie constant.

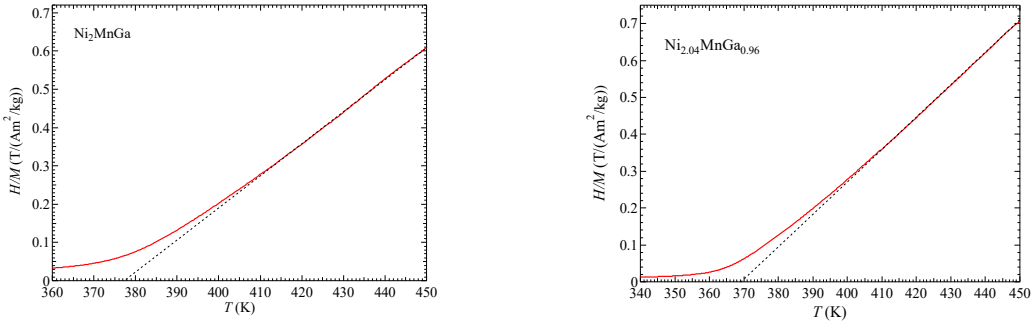


**Figure 2.** Inverse magnetic susceptibilities as: (**a**) $Ni_2MnGa$ and (**b**) $Ni_{2.04}MnGa_{0.96}$. Dotted lines are the fitting lines at the paramagnetic phase.

The Curie constant $C$ is written as:

$$C = \frac{Np_{\text{eff}}^2\mu_B^2}{3k_{\text{B}}} \tag{9}$$

where $N$ is the molecular number per gram. The obtained effective moments $p_{\text{eff}}$ were 4.72 for $Ni_{2.02}MnGa_{0.98}$ and 4.68 for $Ni_{2.04}MnGa_{0.96}$. In Section 3.3, we discuss the itinerant electron ferromagnetism by means of these parameters.

### *3.2. Results of the Magnetic Measurements of Half-Metallic Ferromagnet $Co_2VGa$*

HMFs are comprised of a metallic band for one spin direction. For the other spin direction, a semiconducting band has an energy gap around Fermi energy. $Co_2VGa$ is a HMF with a high spin polarization [16]. It has an $L2_1$-type cubic crystal structure with a lattice constant $a$ = 0.5782 nm. The spin polarization ratio $P$ is defined as:

$$P_0(\%) = \left| \frac{N_\uparrow(E_F) - N_\downarrow(E_F)}{N_\uparrow(E_F) + N_\downarrow(E_F)} \right| \times 100 \tag{10}$$

where $N_\uparrow(E_F)$ and $N_\downarrow(E_F)$ denote the density of states, DOS, at the Fermi energy, $E_F$, in the majority spin ($\uparrow$) and minority spin ($\downarrow$), respectively. Umetsu et al. calculated the DOS by means of the LTMO method with the atomic spheres approximation (ASA). From the results of this calculation, the $P_0$ value ($P$ value at $T$ = 0 K) was 75% and the $P_0$ value of $L2_1$-type $Co_2(V_{1-x}Mn_x)Ga$ alloys ($0 \leq x \leq 1$) was also determined. As for $x$ = 1, $Co_2MnGa$, the obtained spin polarization ratio $P_0$ was 48%. This indicates that $Co_2VGa$ is a higher polarized HMF. The Curie temperatures of $Co_2VGa$ and $Co_2MnGa$ were 337 K and 695 K, respectively. We measured the magnetic field dependences of the magnetization to obtain the magnetic moments, $p_s$, and the spin fluctuation parameters, $T_A$ and $T_0$, and also measured the magnetic susceptibility to obtain the effective magnetic moment, $p_{\text{eff}}$, in the paramagnetic phase. We also obtained $T_A$ and $T_0$ of $Co_2MnGa$ according to the Takahashi theory by means of the magnetization process at 5 K in Reference [16].

Figure 3a shows the permeability of $Co_2VGa$ around the Curie temperature. From the differentiation of the permeability for the temperature, denoted as $dP/dT$, the Curie temperature was obtained as $T_C$ = 337 K. Figure 3b shows the inverse magnetic susceptibility $1/\chi = H/M$ of $Co_2VGa$. The obtained $p_{\text{eff}}$ was 2.06.

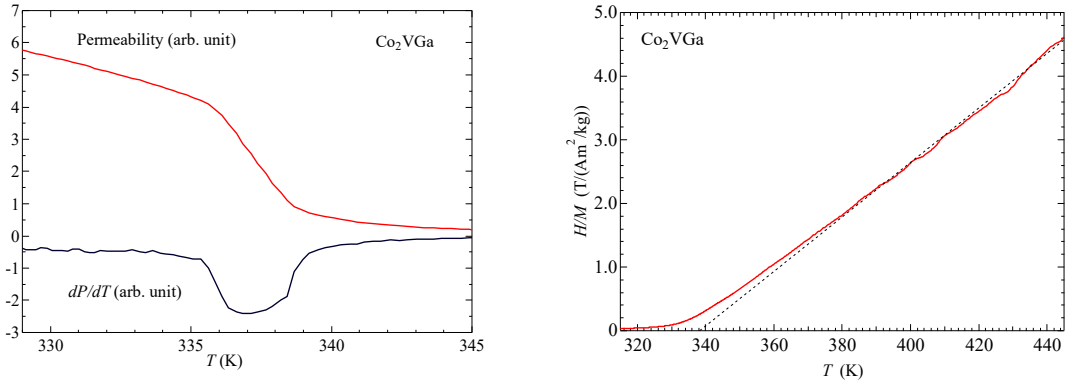


**Figure 3.** (**a**) Permeability of $Co_2VGa$ around the Curie temperature. *dP/dT* indicates the differential of the permeability in the temperature. (**b**) Inverse magnetic susceptibility $1/\chi = H/M$ of $Co_2VGa$. Dotted line is a fitting line at the paramagnetic phase.

Figure 4 shows the $M^3$ vs. $H/M$ plot and $M^4$ vs. $H/M$ plot of $Co_2VGa$ around $T_C$ = 337 K.

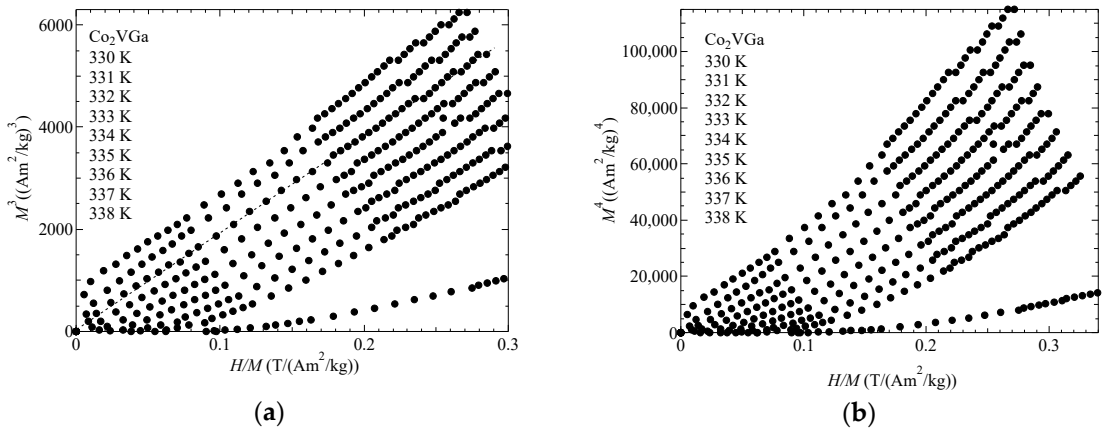


**Figure 4.** The magnetic field dependences of the magnetization of $Co_2VGa$: (**a**) $M^3$ vs. $H/M$; (**b**) $M^4$ vs. $H/M$. Dotted straight line in (a) is a guide for the eyes.

With regard to the Takahashi theory, the magnetization process is expressed as $(H/M) \propto M^4$ by Equation (1) around $T_C$. On the contrary, the $H/M$ was almost proportional to $M^3$ as shown in Figure 4a. Nishihara et al. also measured the magnetization around $T_C$ [17]. The magnetization process at $T_C$ is expressed as $H \propto M^D$ with the index $D = 4.15 \pm 0.05$. Their result was the same as in this study. Nishihara et al. mentioned that the discrepancy between these experimental magnetization results and the Takahashi theory is supposed to arise from the distribution of $T_C$ in the sample because the fourth-order expansion of the magnetic-free energy vanishes at the Curie temperature. In this study, we tried again with other ingots from the former sample used by Nishihara et al. As this experiment reproduced the former experiment, there may be an essential reason. Incidentally, other magnetic models have indicated that the molecular field theory denotes the $D$ value as 3.0, the three-dimensional Heisenberg model denotes the $D$ value as 4.8, and the three dimensional Ising model as 4.82 [18]. None of these matched the analysis in this investigation. In order to obtain the spin fluctuation parameters $T_A$ and $T_0$ of $Co_2VGa$, we measured the magnetization process of $Co_2VGa$ at 5 K. Figure 5 shows the Arrott plot ($M^2$ vs. $H/M$) of $Co_2VGa$. The parameter $F_1$ was obtained by applying the slope value of the Arrott plot to Equation (4). The parameters $T_A$ and $T_0$ were derived by Equations (5) and (6). The obtained $T_A$ and $T_0$ were 2258 K and 213 K, respectively.

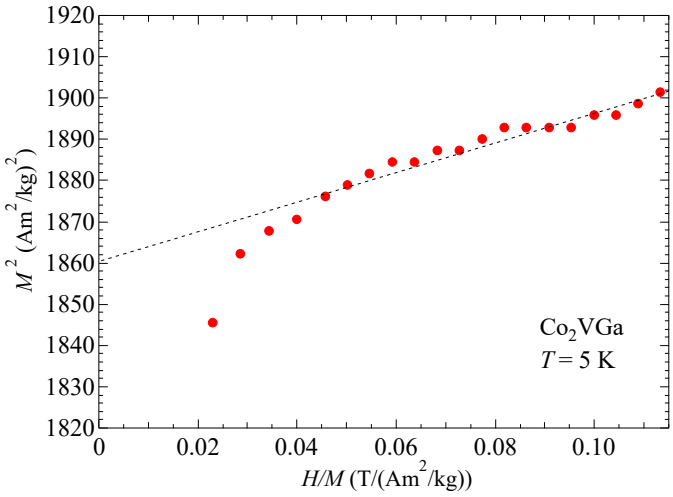


**Figure 5.** The Arrott plot ($M^2$ vs. $H/M$) of $Co_2VGa$ at $T$ = 5 K.

### *3.3. Analysis According to the Takahashi Theory*

Table 2 indicates the Curie temperature $T_C$, the effective magnetic moment $p_{eff}$, the spontaneous magnetization $p_S$, the magnetic moment ratio $p_{eff}/p_S$, the spin fluctuation parameters $T_A$ and $T_0$, the critical temperature ratio $T_C/T_0$, and $k_m$, as obtained from Equation (8).

**Table 2.** Basic magnetic parameters and $k_m$ as obtained from Equation (8).

| | $T_C$ (K) | $p_{eff}$ ($\mu_B$) | $p_S$ ($\mu_B$) | $p_{eff}/p_S$ | $T_A$ (K) | $T_0$ (K) | $T_C/T_0$ | $k_m$ | Reference [1] |
|---|---|---|---|---|---|---|---|---|---|
| $Ni_2MnGa$ | 375 | 4.75 * | 3.93 | 1.21 | 563 | 245 | 1.53 | 1.61 | This work *, [9] |
| $Ni_{2.02}MnGa_{0.98}$ | 372 | 4.72 * | 3.79 | 1.25 | 566 | 288 | 1.29 | 1.48 | This work *, [9] |
| $Ni_{2.04}MnGa_{0.96}$ | 366 | 4.68 * | 3.64 | 1.28 | 567 | 345 | 1.06 | 1.34 | This work *, [9] |
| $Co_2VGa$ | 337 | 2.06 | 1.87 | 1.10 | 2258 | 213 | 1.58 | 1.50 | This work |
| $Co_2MnGa$ | 695 | 4.16 | 4.09 | 1.02 | 1,037 | 364 | 1.91 | 1.57 | [16,19] |
| Ni | 623 | 3.3 | 0.6 | 5.5 | $1.76 \times 10^4$ | $4.83 \times 10^3$ | 0.129 | 1.41 | [13] |
| MnSi | 30 | 2.25 | 0.4 | 5.6 | $2.18 \times 10^3$ | 155 | 0.194 | 1.88 | [7,10] |
| $Ni_3Al$ | 41.5 | 1.3 | 0.075 | 17.3 | $3.67 \times 10^4$ | $2.76 \times 10^3$ | 0.015 | 1.06 | [7,20] |
| $Y(Co_{0.85}Al_{0.15})_2$ | 26 | 2.15 | 0.138 | 15.6 | $7.26\times 10^3$ | $1.41\times 10^3$ | 0.018 | 1.08 | [7,21] |
| $ZrZn_2$ | 21.3 | 1.44 | 0.12 | 12 | $7.4\times 10^3$ | 1390 | 0.015 | 0.74 | [7,22] |
| $CoS_2$ | 120 | 1.72 | 0.98 | 1.76 | $2.20\times 10^3$ | 294 | 0.41 | 0.96 | [12,23] |
| UCoGe | 2.4 | 1.93 | 0.039 | 49.5 | $5.92 \times 10^3$ | 362 | 0.0065 | 1.74 | [7,24] |
| $UGe_2$ | 52.6 | 3.00 | 1.41 | 2.13 | 442 | 92.2 | 0.571 | 1.61 | [14] |
| $NpFe_4P_{12}$ | 23 | 1.55 | 1.35 | 1.15 | 285 | 16.4 | 1.40 | 1.44 | [14,25] |

[1] Citations in our published paper [9] are incorrect. The correct citations are listed above. We apologize for this mistake. * These values were obtained by this work.

The $k_m$ value was around 1.4. Figure 6 shows the generalized Rhodes–Wohlfarth plot using the parameters in Table 2 [7,26]. The points of $Ni_{2+x}MnGa_{1-x}$ are in accordance with the dotted line as $k_m$ = 1.4. It is noteworthy that the HMFs, $Co_2VGa$ and $Co_2MnGa$, were also in accordance with this line. Originally, the Takahashi theory was applied to weak ferromagnets. It is interesting that this theory can be applied to strongly correlated 5*f* electron systems as well as Heusler HMFs.

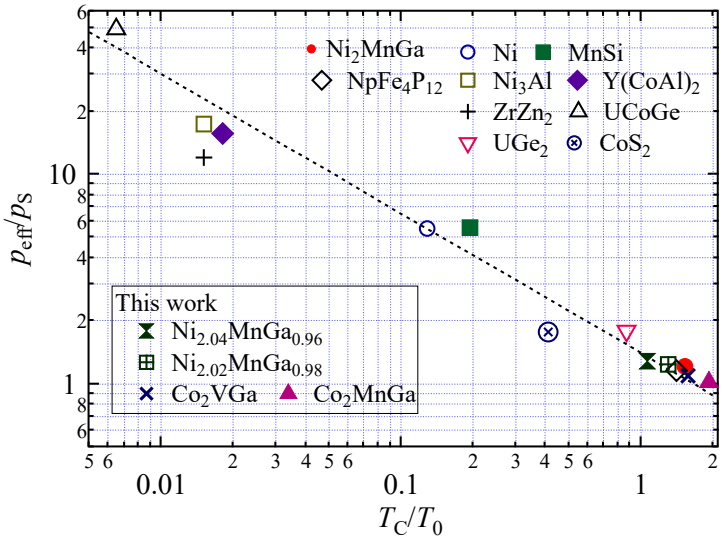


**Figure 6.** The generalized Rhodes–Wohlfarth plot (double logarithmic plot of $p_{eff}/p_S$ and $T_C/T_0$) for this work and other notable alloys and compounds. The dotted line indicates $k_m$ = 1.4 as obtained from Equation (8).

### *3.4. Comparison between the Spontaneous Magnetic Moment at the Ground State, $p_S$, and the Paramagnetic Magnetic Moment, $p_C$, for HMFs*

In this subsection, we consider the magnetism of Heusler alloys by comparing the spontaneous magnetic moment at the ground state and paramagnetic magnetic moment.

We rewrote the definitions of $p_S$, $p_{sat}$, $p_{eff}$, and $p_C$ to make the following argument plain. $p_S$ is the spontaneous magnetic moment at the ground state ($T$ = 0 K or $T << T_C$). $p_{sat}$ is the saturation magnetic moment at the ground state ($T$ = 0 K or $T << T_C$). $p_{eff}$ is the effective magnetic moment in the paramagnetic phase. $p_C$ is the magnetic moment in the paramagnetic phase. These four magnetic moments are defined by the unit of $\mu_B$. The relation between $p_{eff}$ and $p_C$ is described as

$$p_{eff} = \sqrt{p_C(p_C + 2)} \tag{11}$$

In HMFs, the band for minority spin electrons has a gap at the Fermi level and indicates semi-metallic bands. On the other hand, for majority spin electrons, the Fermi level intersects the bands and represents metallic bands. Table 3 represents the magnetic parameters of ferromagnetic Heusler alloys, with the paramagnetic moment $p_C$. The notable point of Table 3 is that the $p_C/p_s$ of $Ni_2MnGa$ and many half-metallic Heusler alloys were smaller than 1. From Equation (9) and (11), the $p_C$ is calculated by the Curie constant, $C = N\mu_{eff}^2/3k_B = Np_{eff}^2\mu_B^2/3k_B = Np_C(p_C + 2)\mu_B^2/3k_B$. $p_C$ refers to the magnetic moment in the paramagnetic phase deduced from the Curie constant C. $p_c/p_s$ is 1 for the local moment ferromagnetism. For the weak itinerant electron ferromagnetism, the $p_c/p_s$ is larger than 1 [7].

As for $Ni_2MnGa$, $p_{eff}$ was 4.75, as shown in Table 3. Therefore, the $p_c$ obtained was 3.85 from Equation (11), and the $p_C/p_S$ value was 0.980. As a result, the $p_C/p_S$ was a little smaller than 1. Webster et al. compared the magnetic moment obtained by the saturation magnetization measurement where $p_{sat}$ = 4.17 [15]. Then, the $p_{sat}/p_s$ was 0.92. The magnetization of $Ni_2MnGa$ in the magnetic field of 5.0 T at 5 K was 4.10 $\mu_B$/f.u. Therefore, the $p_{sat}/p_s$ was 0.96. Regarding the half-metallic Heusler alloys, $Co_2VGa$ and $Co_2MnGa$, which are the focus of this article, the $p_{sat}/p_s$ were 0.70 and 0.80, respectively. The renowned half-metallic Heusler alloys and compounds listed in Table 3 indicate the property of $p_C/p_S < 1$. The magnetic properties of the inter-metallic compounds CoMnSb, NiMnSb, PtMnSb, $Pd_2MnSn$, and $Pd_2MnSb$ showed an effective paramagnetic moment above $T_C$, which was also smaller than the spontaneous and saturation moment of the ground state at $T$ = 0 K [27,28].

As above-mentioned, the spin polarization values $P_0$ of $Co_2VGa$ and $Co_2MnGa$ were 75% and 48%, respectively [16]. This indicates that $Co_2VGa$ is a higher polarized HMF. The $p_C/p_S$ values of $Co_2VGa$ and $Co_2MnGa$ were 0.70 and 0.80, respectively, as shown in Table 3. The results concerned with these two alloys indicate that the alloy with a larger spin polarization showed a smaller $p_C/p_S$ value.

Dong et al. studied the spin polarization of $Co_2MnGe$ experimentally and analyzed the temperature dependence of the spin polarization [29] where the spin polarization of $Co_2MnGe$ was 27% at 2 K. However, the spin polarization decreased with increasing temperature and vanished at 300 K. It is considered that the magnetic moment decreases at a high temperature with the decrease of the spin polarization. Ott et al. also suggested that this effect could be attributed to a decrease of the conduction electron spin polarization in the paramagnetic phase, which has a higher temperature than $T_C$ [27]. A simple molecular field model, which took into account both local moments and spin-polarized itinerant electrons, explained that $p_C/p_S < 1$ [27]. They introduced an "Enhanced Temperature-independent Pauli susceptibility", which comes from the itinerant electron bands intersecting the Fermi level, and explained that the Curie constant was reduced if the interactions between local magnetic moments and holes were antiferromagnetic. Therefore, the reduction in the Curie constant indicates that the magnetic moment $p_C$ at a high temperature in a paramagnetic phase is smaller than that of the spontaneous magnetization $p_S$ as well as the saturation moment $p_{sat}$ at the ground phase of $T$ = 5 K. Webster et al. pointed out the electronic and spin phases of $Ni_2MnGa$ [15]. In the paramagnetic phase, only the Mn atoms carry a magnetic moment. It is supposed that in the paramagnetic phase a large moment was induced by the electrons around the Mn atom at the Mn site. On the contrary, at the Ni site, the spins fluctuated at high temperature in the paramagnetic phase. Therefore, it is also supposed that $p_C$ at a high temperature in the paramagnetic phase is smaller than that of the $p_S$. As for $Co_2VGa$ and $Co_2MnGa$, which were treated in this article, it is of interest to investigate the temperature dependence of the spin polarization experimentally.

**Table 3.** Magnetic parameters of ferromagnetic Heusler alloys. $p_C$ indicates the magnetic moment at the paramagnetic phase. The relation between $p_{eff}$ and $p_C$ is defined by the equation of $p_{eff} = \sqrt{p_C(p_C+2)}$.

| Sample | $T_C$ (K) | $p_S$ ($\mu_B$/f.u.) | $p_{eff}$ ($\mu_B$/f.u.) | $p_C$ ($\mu_B$/f.u.) | $p_C/p_S$ | Reference |
|---|---|---|---|---|---|---|
| $Ni_2MnGa$ | 375 | 3.93 | 4.75 * | 3.85 | 0.980 | This work *, [9] |
| $Ni_{2.02}MnGa_{0.98}$ | 372 | 3.79 | 4.72 * | 3.82 | 1.01 | This work *, [9] |
| $Ni_{2.04}MnGa_{0.96}$ | 366 | 3.64 | 4.68 * | 3.79 | 1.04 | This work *, [9] |
| $Co_2VGa$ | 337 | 1.87 | 2.06 | 1.30 | 0.70 | This work |
| $Co_2MnSi$ | 1034 | 5.01 | 2.86 | 2.03 | 0.41 | [30] |
| $Co_2MnGe$ | 905 | 4.76 | 3.70 | 2.82 | 0.56 | [30] |
| $Co_2MnSn$ | 825 | 5.02 | 5.29 | 4.38 | 0.87 | [31] |
| $Co_2MnGa$ | 695 | 4.09 | 4.16 | 3.28 | 0.80 | [19] |
| $Co_2FeSi$ | 1015 | 5.42 (300 K) | 5.65 | 4.74 | 0.875 | [32] |
| $Co_2FeGa$ | 1089 | 5.05 (300 K) | 4.59 | 3.69 | 0.730 | [32] |
| CoMnSb | 478 | 4.2 | 4.0–4.6 | 3.1-3.7 | 0.74–0.88 | [27] |
| NiMnSb | 728 | 4.2 | 2.9–4.2 | 2.1-3.3 | 0.69–0.79 | [27] |
| PtMnSb | 572 | 3.96 | 4.3–4.9 | 3.4-4.0 | 0.86–1.01 | [27] |
| $Ni_2MnIn$ | 315 | 4.4 | 4.69 | 3.80 | 0.86 | [33,34] |
| $Rh_2MnSn$ | 410 | 4.14 | 4.83 | 3.93 | 0.95 | [31] |
| $Pd_2MnSn$ | 189 | 4.23 | 4.70 | 3.81 | 0.90 | [28] |
| $Pd_2MnSb$ | 255 | 4.40 | 4.8 | 3.9 | 0.89 | [28] |

* These values were obtained by this work.

In Figure 6, the HMFs of $Co_2VGa$ and $Co_2MnGa$ were in accordance with the generalized Rhodes–Wohlfarth plot with a $k_m$ around 1.4. The majority of the bands of these two alloys intersected the Fermi level [16]. Therefore, the magnetic property of the itinerant electron appeared in the majority bands and was confirmed by Takahashi's theory.

## 4. Conclusions

In this article, experimental investigations and discussions into the field dependence of magnetization and temperature dependences of magnetic susceptibility in $Ni_{2+x}MnGa_{1-x}$ ($x$ = 0.00,

0.02, 0.04), $Co_2VGa$, and $Co_2MnGa$ Heusler alloy ferromagnets were performed following the spin fluctuation theory of itinerant electron ferromagnetism by Y. Takahashi.

1. As for $Ni_{2+x}MnGa_{1-x}$, the spin fluctuation parameters in *k*-space (momentum space, $T_A$) and that in energy space ($T_0$) obtained at $T_C$ and 5 K were almost the same within ±10% error. This consequently indicates that the spin fluctuation parameters can be obtained from the *H*/*M* vs. $M^4$ plot at $T_C$ and also from an Arrott plot (*H*/*M* vs. $M^2$) at a low temperature of $T << T_C$.
2. As for $Co_2VGa$, the *H* vs. $M^5$ dependence was not shown at $T_C$. $T_A$ and $T_0$ were obtained by means of an Arrott plot at 5 K, which is well below $T_C$ = 337 K;
3. In order to obtain a $k_m$ value as defined in Equation 8, the magnetic susceptibility was measured, and the $p_{eff}$ was obtained by means of Curie law. The $k_m$ of $Co_2VGa$ (1.50) and $Co_2MnGa$ (1.57) were around 1.4, which was proposed in Takahashi's theory. The generalized Rhodes–Wohlfarth plot of $p_{eff}/p_S$ versus $T_C/T_0$ indicated that the relationship between $p_{eff}/p_S$ and $T_0/T_C$ for the ferromagnets, including $Ni_{2+x}MnGa_{1-x}$ and HMFs of $Co_2VGa$ and $Co_2MnGa$, followed Takahashi's theory. In HMFs, the band for minority spin electrons has a gap at the Fermi level and indicates semi-metallic bands. On the other hand, for majority spin electrons, the Fermi level intersects the bands and represents metallic bands. The magnetic properties of the itinerant electron of these two HMFs alloys appeared in the majority bands and were confirmed by Takahashi's theory;
4. As for $Ni_{2+x}MnGa_{1-x}$ and HFMs, we obtained the spontaneous magnetic moment at the ground state, $p_S$, by an Arrott plot at 5 K, and the high temperature magnetic moment, $p_C$, at the paramagnetic phase. The $p_C/p_S$ was smaller than 1 for many Heusler alloys, which is a different property from the localized ferromagnets ($p_C/p_S$ = 1), or, for weak itinerant electron ferromagnets ($p_C/p_S$ > 1). A comparison between $Co_2VGa$ and $Co_2MnGa$ indicates that the alloy with a larger spin polarization showed a smaller $p_C/p_S$ value. Further, an experimental investigation into the temperature dependence of spin polarization is needed to clarify the mechanism of shrinkage of the magnetic moments in the paramagnetic phase at a high temperature.

**Author Contributions:** Sample preparation, D.L., F.H., X.X., R.Y.U, G.O., and T.E.; Investigation, T.S., Y.H., A.F., X.X., R.Y.U., and T.E.; Writing—original draft preparation, T.S, Y.H., and A.F.; Writing—review and editing, T.S. and T.K.; Supervision, T.K.

**Funding:** This research received no external funding.

**Acknowledgments:** We would like to thank Hironori Nishihara for participating in fruitful discussions. This project was partly supported by the Ryukoku Extension Center (REC) at Ryukoku University. This research was carried out in part at the International Research Center for Nuclear Materials Science, Institute for Materials Research, Tohoku University.

**Conflicts of Interest:** The authors declare no conflict of interest.

## References

1. Moriya, T. *Spin Fluctuations in Itinerant Electron Magnetism*; Springer: Berlin, Germany, 1985; ISBN 978-3-642-82499-9.
2. Moriya, T.; Kawabata, A. Effect of Spin Fluctuations on Itinerant Electron Ferromagnetism. *J. Phys. Soc. Jpn.* **1973**, *34*, 639–651. [CrossRef]
3. Moriya, T.; Kawabata, A. Effect of Spin Fluctuations on Itinerant Electron Ferromagnetism. II. *J. Phys. Soc. Jpn.* **1973**, *35*, 669–676. [CrossRef]
4. Takahashi, Y. On the origin of the Curie Weiss law of the magnetic susceptibility in itinerant electron ferromagnetism. *J. Phys. Soc. Jpn.* **1986**, *55*, 3553–3573. [CrossRef]
5. Takahashi, Y. Theoretical Development in Itinerant Electron Ferromagnetism. *J. Phys. Conf. Ser.* **2017**, *868*, 012002. [CrossRef]
6. Takahashi, Y.; Nakano, H. Magnetovolume effect of itinerant electron ferromagnets. *J. Phys. Cond. Matter.* **2006**, *18*, 521. [CrossRef]

7. Takahashi, Y. *Spin Fluctuation Theory of Itinerant Electron Magnetism*; Springer: Berlin, Germany, 2013; ISBN 978-3-642-36666-6.
8. Sakon, T.; Hayashi, Y.; Fujimoto, N.; Kanomata, T.; Nojiri, H.; Adachi, Y. Forced magnetostriction of ferromagnetic Heusler alloy $Ni_2MnGa$ at the Curie temperature. *J. Appl. Phys.* **2018**, *123*, 213902. [CrossRef]
9. Sakon, T.; Hayashi, Y.; Li, D.X.; Honda, F.; Oomi, G.; Narumi, Y.; Hagiwara, M.; Kanomata, T.; Eto, T. Forced Magnetostrictions and Magnetizations of $Ni_{2+x}MnGa_{1-x}$ at Its Curie Temperature. *Materials* **2018**, *11*, 2115. [CrossRef]
10. Matsunaga, M.; Ishikawa, Y.; Nakajima, T. Magneto-volume effect in the weak itinerant ferromagnet MnSi. *J. Phys. Soc. Jpn.* **1982**, *51*, 1153. [CrossRef]
11. Rizal, C.; Kolthammer, J.; Pokharel, R.K.; Choi, B.C. Magnetic properties of nanostructured Fe-Co alloys. *J. Appl. Phys.* **2013**, *113*, 113905. [CrossRef]
12. Nishihara, H.; Harada, T.; Kanomata, T.; Wada, T. Magnetization process near the Curie temperature of an itinerant ferromagnet $CoS_2$. *J. Phys. Conf. Ser.* **2012**, *400*, 032068. [CrossRef]
13. Nishihara, H.; Komiyama, K.; Oguro, I.; Kanomata, T.; Chernenko, V. Magnetization processes near the Curie temperatures of the itinerant ferromagnets, $Ni_2MnGa$ and pure nickel. *J. Alloys Compd.* **2007**, *442*, 191–193. [CrossRef]
14. Tateiwa, N.; Pospíšil, J.; Haga, Y.; Sakai, H.; Matsuda, T.D.; Yamamoto, E. Itinerant ferromagnetism in actinide 5*f*-electron systems: Phenomenological analysis with spin fluctuation theory. *Phys. Rev. B* **2017**, *96*, 035125. [CrossRef]
15. Webster, P.J.; Ziebeck, K.R.A.; Town, S.L.; Peak, M.S. Magnetic order and phase transition in $Ni_2MnGa$. *Philos. Mag. B.* **1984**, *49*, 295–310. [CrossRef]
16. Umetsu, R.Y.; Kobayashi, K.; Fijita, A.; Kainuma, R.; Ishida, K.; Fukamichi, K.; Sakuma, A. Magnetic properties, phase stability, electric structure, and half-metallicity of $L2_1$-type $Co_2$ $(V_{1-x}Mn_x)Ga$ Heusler alloys. *Phys. Rev. B* **2008**, *77*, 104422. [CrossRef]
17. Nishihara, H.; Furutani, Y.; Wada, T.; Kanomata, T.; Kobayashi, K.; Kainuma, R.; Ishida, K.; Yamauchi, T. Magnetization Process near the Curie Temperature of a Ferromagnetic Heusler Alloy $Co_2VGa$. *J. Supercond. Nov. Magn.* **2011**, *24*, 679–681. [CrossRef]
18. Seeger, M.; Kaul, S.N.; Kronmüller, H.; Reisser, R. Asymptotic critical behavior of Ni. *Phys. Rev. B* **1995**, *51*, 12585. [CrossRef]
19. Ido, H.; Yasuda, S. Magnetic properties of Co-Heusler and related mixed alloys. *J. Phys. Colloques (Paris)* **1988**, *49*, C8-141–C8-142. [CrossRef]
20. De Boer, F.R.; Biesterbos, J.; Schinkel, C.J. Ferromagnetism in the intermetallic phase $Ni_3Al$. *Phys. Lett. A* **1969**, *24*, 355–357. [CrossRef]
21. Yoshimura, K.; Takigawa, M.; Takahashi, Y.; Yasuoka, H.; Nakamura, Y. NMR Study of Weakly Itinerant Ferromagnetic $Y(Co_{1-x}Al_x)_2$. *J. Phys. Soc. Jpn.* **1987**, *56*, 1138–1155. [CrossRef]
22. Ogawa, S. Electrical Resistivity of Weak Itinerant Ferromagnet $ZrZn_2$. *J. Phys. Soc. Jpn.* **1976**, *40*, 1007–1009. [CrossRef]
23. Miyahara, S. Magnetic Properties of $FeS_2$ and $CoS_2$. *J. Appl. Phys.* **1968**, *39*, 896–897. [CrossRef]
24. Sato, N.K.; Deguchi, K.; Imura, K.; Kabeya, N.; Tamura, N.; Yamamoto, K. Correlation of Ferromagnetism and Superconductivity in UCoGe. *AIP Conf. Proc.* **2011**, *1347*, 132–137. [CrossRef]
25. Aoki, D.; Haga, Y.; Homma, Y.; Sakai, H.; Ikeda, S.; Shiokawa, Y.; Yamamoto, E.; Nakamura, A.; Onuki, Y. First single crystal growth of the Transuranium filled-Skutterudite compound $NpFe_4P_{12}$ and its magnetic and electrical properties. *J. Phys. Soc. Jpn.* **2006**, *75*, 073073. [CrossRef]
26. Rhodes, P.; Wohlfarth, E.P. The effective Curie-Weiss constant of ferromagnetic metals and alloys. *Proc. Roy. Soc. A* **1963**, *273*, 247–258. [CrossRef]
27. Otto, M.J.; van Woerden, R.A.M.; van der Valk, P.J.; Wijngaard, J.; van Bruggen, C.F.; Haas, C.; Buschow, K.H.J. Half-metallic ferromagnets. I. Structure and magnetic properties of NiMnSb and related inter-metallic compounds. *J. Phys. Cond. Mater.* **1989**, *1*, 2341–2350. [CrossRef]
28. Webster, P.J.; Ramadan, M.R.I. Magnetic order in Palladium-based Heusler alloys Part 1: $Pd_2MnIn_{1-x}Sn_x$ and $Pd_2MnIn_{1-x}Sb_x$. *J. Magn. Magn. Mater.* **1977**, *5*, 51–59. [CrossRef]
29. Dong, X.Y.; Adelmann, C.; Xie, J.Q.; Palmstrøm, C.J.; Low, X.; Strand, J.; Crowell, P.A.; Barnes, J.-P.; Petford-Long, A.K. Spin injection from the Heusler alloy $Co_2MnGe$ into $Al_{0.1}Ga_{0.9}As$/GaAs heterostructures. *Appl. Phys. Lett.* **2005**, *86*, 102107. [CrossRef]

30. Ido, H. Induced magnetic moment on Co below $T_C$ in the ferromagnetic Heusler-type alloys $Co_2MnX$ (X = Si, Ge and Sn). *J. Magn. Magn. Mater.* **1986**, *54–57*, 937–938. [CrossRef]
31. Uhl, E. Magnetization of two new series of Heusler alloys: $(Rh_{1-x}Co_x)_2MnSn$ and $(Rh_{1-x}Ni_x)_2MnSn$. *J. Magn. Magn. Mater.* **1985**, *49*, 101–105. [CrossRef]
32. Deka, B.; Chakraborty, D.; Srinivasan, A. Magnetic properties of $Co_2Fe(Ga_{1-x}Si_x)$ alloys. *Physica B* **2014**, *448*, 173–176. [CrossRef]
33. Kanomata, T.; Shirakawa, K.; Kaneko, T. Effect of hydrostatic pressure on the Curie temperature of the Heusler alloys $Ni_2MnZ$ (Z = Al, Ga, In Sn and Sb). *J. Magn. Magn. Mater.* **1987**, *65*, 76–82. [CrossRef]
34. Webster, P.J. Heusler alloys. *Contemp. Phys.* **1969**, *10*, 559–577. [CrossRef]